Vol. 1 No.1, July 2021

FUAM Journal of Pure and Applied Science

Available online at
www.fuamjpas.org.ng

An official Publication of
College of Science
Joseph Sarwuan Tarka University,
Makurdi.

FUAM Journal of Pure and Applied Science
© College of Science, Joseph Sarwuan Tarka University, Makurdi
https://fuamjpas.org.ng/
Vol.1. No. 1. July, 2021

Growth Mechanism and Structural Elucidation of Indium Oxide Microstructures Prepared by Carbothermal and Hydrogen Reduction Processes

[2*]P.R. Jubu, [1, 3] T.M. Aper and [2]V.M. Igba

[1]School of Physics, Universiti Sains Malaysia, 11800USM, Pinang, Malaysia.
[2]Department of Physics, Joseph Sarwuan Tarka University Makurdi (JOSTUM), P.M.B. 2373 Makurdi, Benue State, Nigeria.
[3]Department of Physics, Benue State University (BSU), P.M.B. 102119, Makurdi, Benue State, Nigeria.
Correspondence E-mails: jubu_raphael@yahoo.com ; peverga.jubu@uam.edu.ng

Received: 19/04/2021 **Accepted**: 14/07/2021 **Published online**: 24/07/2021

Abstract

In this study, the growth mechanism for the deposition of pure In_2O_3 crystal and indium-In_2O_3 mixed-phase films is proposed for the carbothermal and hydrogen reduction growth processes, respectively. X-ray diffractograms confirm the formation of the pure In_2O_3crystal and indium-In_2O_3 mixed-phase films. Surface morphology observation show pure microaggregates for the pure In_2O_3 film, and a combination of microclusters and microspheres for the mixed-phase film. The initially condensed seed-layer in the form of small solid-crystals and liquid-catalyst, serving as nucleation sites are suggested to result to the development of the pure and indium-In_2O_3 mixed-phase films for the carbo-thermal and hydrogen reduction growth processes, respectively. Composition analyses reveal rich- and deficient oxygen contents for the pure and mixed phase films, respectively thus, supporting the X-ray diffraction results. Optical bandgaps values are found to be 3.07 and 3.85 eV for the pure In_2O_3 and mixed phase films, respectively. The carbothermal reduction technique has been found to be more appropriate for the growth of pure In_2O_3 crystal.

Keywords: Indium oxide, Reducing ambient, Chemical vapour deposition, Growth mechanism.

Introduction

Fabrication of indium oxide (In_2O_3) nanostructures (NSs) has received great attention due to their novel characteristics and promise for application in gas sensors[1, 2], light emitting diodes, nanoscale transistors, photodetectors and catalysts [2, 3]. Up to date, many techniques have been deployed to develop various In_2O_3 NSs [1-5] for different applications. The synthesis technique and processing parameters can affect the size, morphology and composition of In_2O_3 films [2]. The morphology in turn can greatly influence the properties of NSs and determines the best device application [3].

Chemical vapour deposition (CVD) is afacile and very convenient method for producing diverse dense array of NSs with different morphologies, owing to its many synthesis parameters such as temperature, chamber pressure, precursor type, gas flow rate, growth ambient, and substrate-source distance. Among the various CVD types, the reducing-ambient CVD (RA-CVD) is preferred because of its eco-friendliness, availability, and cost-effective precursor (oxide powder). However, In_2O_3 powder has a high melting point about 1900 ℃, and requires high evaporating temperature. On the contrary, other precursors which have lower melting point such as $GaCl_3$ (for atmospheric pressure CVD (APCVD) and mist CVD (MCVD)) [5], metallic indium (for APCVD or thermal CVD (TCVD))[2], trimethylindium and

triethylindium (for metal-organic CVD and aerosol-assisted CVD) could be either corrosive to CVD metal parts, more costly, or environmentally unfriendly as compared to In_2O_3 powder (for RA-CVD).

Thermal evaporation and deposition of In_2O_3 NSs from its oxide powder source requires high temperature about 1300–1500 ℃under atmospheric pressure [6, 7]. However, the use of a reducing ambient usually lowers the evaporation temperature (down to about 750–1000 ℃) for easy melt[5, 8]. Another CVD technique that drastically reduces the melting point of In_2O_3 powder (down to about 700 ℃) is the low-pressure CVD[9].Nevertheless, this method is considered complex, energy consuming and costly because of the vacuum pump required to pump down the chamber pressure. Therefore, the commonest and cost-effective CVD technique is the RA-CVD which uses a reducing agent to lower the evaporating point of In_2O_3 powder. Several reductants such as ethanol [8], hydrazine hydrate (N_2H_4) [4], H_2, NH_3, and H_2S [9, 10] have been recommended for promoting the evaporation of metal oxides in CVD. However, film synthesized by NH_3, H_2S, ethanol and N_2H_4 reduction may lead to contamination with N,S, or C doping, which may affect device performance[1]. Carbon from charcoal or graphite is the commonest reducing agent for the RA-CVD [4, 11, 12], owing to its easy availability and cost-effectiveness.

Synthesis of In_2O_3 films by RA-CVD techniques such as carbothermal reduction (CTR) and hydrogen reduction (HR) at temperature below 1000 ℃ can be facile, faster and energy-saving. The known growth mechanism for direct deposition of films on a bare/or seed-free substrate is the vapour-solid process (VS).

The present paper reports the fabrication of In_2O_3 microstructures (MSs) on an unseeded Si substrate by the CTR and HR CVD processes. It is noted that the mechanism for the formation of indium-In_2O_3 mixed-crystal system is rarely reported in the literature [7, 13-15].The usual VS growth mechanism governing the direct deposition of films on a seed-free template has been slightly modified to explain the formation of the produced pure and indium-In_2O_3 mixed-phase films reported in this work.

Materials and Methods

The In_2O_3 samples are prepared in two different reducing growth ambientes. For the CTR, a ceramic boat with a 1:1 mixture of In_2O_3 and activated carbon powder is inserted to the center of the furnace, while p-type Si (100) substrate (size: 1× 1.5 cm) is placed at a separation 26 cm downstream from the source boat. Meanwhile, the furnace is degassed by flowing 600 sccm N_2 gas for 20 min.

Temperature of the furnace is ramped at 15 ℃/minto 850 °Cand maintained for 60 min reaction time while supplying water vapour into the reactor by diverting the flowing N_2through a water bubbler held at 65 ℃. Water vapouris used a source of oxygen. The furnace is shot down after the 60 min dwell time and a yellowish-white coating can be seen on the substrate and inner walls of the quartz tube. On the contrary, for the HR, In_2O_3 powder is used without carbon as the reductant while keeping the other synthesis parameters same, as described for the CTR and deposition process.100 sccm hydrogen gas is supplied into the reactor from the upstream through a separate pipeline as the reducing gas. The produced film is gray in colour, indicating the presence of metallic indium [4, 5].

The crystalline phase is investigated by high-resolution X-ray diffraction (HR-XRD, PANalytical X'pert Pro) using Cu-Kα (λ=1.54060 Å) radiation in the 2θ range 25–65° with step size 0.02° in Bragg-Brentano geometry. Surface morphology is observed using field-emission scanning electronic microscope (FE-SEM, Nano SEM 450 FEI Nova) at 10 kV. Optical diffused reflectance is measured by UV-vis-NIR spectrophotometer (Cary 5000, Agilent Tech.).

Results and Discussion

Structural characterization

Fig. 1 illustrates XRD patterns of the In_2O_3 MSs produced in different reducing atmospheres. The film prepared by CTR (pattern 'a') exhibit intense In_2O_3 diffraction peaks indexed to cubic In_2O_3 phase [8] (JCPDS card no. 00-044-1087).No peaks belonging to another phase can be detected. In the other hand, the film synthesized by HR show relatively low diffraction peaks which can be indexed to cubic In_2O_3 phase marked by the prefixed 'IO' and tetragonal metallic indium phase marked by the prefixed 'I' (JCPDS card no. 01-085-1409).The percentage fraction of the tetragonal indium and cubic In_2O_3 phases are estimated to be 91% and 9%, respectively, suggesting that the former crystal phase is dominant on the produced film. The higher percentage phase fraction (91%) for the metallic indium can be seen on the higher numbers of indium diffraction peaks and intensity. It is known that the number of peaks and/ or higher XRD intensity is an indication for the dominance of the amount of a material or phase. Meanwhile, the loss of intensity for the In_2O_3 peaks can be observed for the film prepared by HR, except for the IO (321) plane. A similar observation is reported by Guenther *et al.* [16] when the yannealedindium-tin-oxide at 450 ℃ in H_2 atmosphere. Metallic indium diffraction peaks are also reported in their study. The change in preferred growth orientation can be attributed to the different growth mechanisms governing the CTR and HR processes, and also due to the different materials phases.

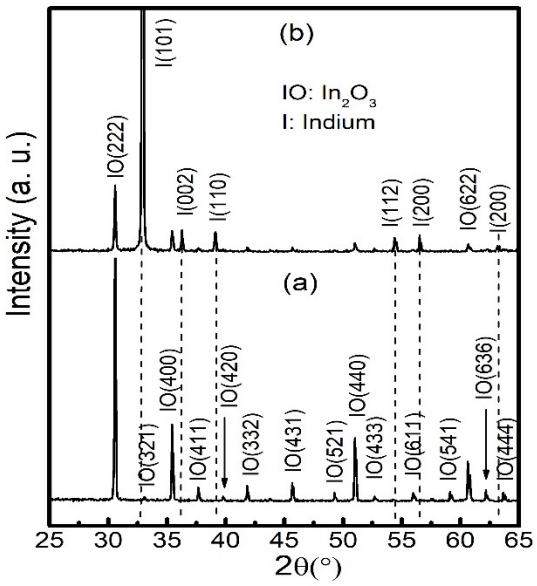

Figure 1. Typical XRD patterns of the In_2O_3 MSs deposited by: (a) CTR (b) HR.

X-ray diffraction peak profile analysis is carried out on the preferred growth directions IO (222) and I(101) for the MSs deposited by the CTR and HR methods, respectively. Crystallite size D is determined using Debye Scherrer formula, $D = 0.9\lambda/\beta\cos\theta$, while the microstrain ε is estimated by the relation $\varepsilon = \beta/4\tan\theta$, where β is full width at half maxima(FWHM) in radians, θ is peak position, λ is X-ray wavelength (= 0.15406 nm) [5]. The film produced by CTR is found to have bigger value of D (75.01 nm)as compared to the value 53.13nmfor the HR-grown film. The relatively bigger and smaller D for the CTR- and HR-grown films can be traced to the difference in the diffraction line broadening $1.903\times 10^{-3}$and 2.699×10^{-3} rad, respectively. Meanwhile, the $\varepsilon$is found to be 1.943×10^{-3} and 2.555×10^{-3}, which can be ascribed to the narrower and wider FWHM for the CTR- and HR-produced MSs, respectively. It can be observed that D and ε are indirectly related: The higher the strain on the crystal, the smaller is the value of D and vice versa. This indicates that diffraction line wide/ broadening can be due to the sum of contributions from D and εpresent in the material.

Morphology characterization

Fig.2 shows surface morphology of the In_2O_3MSs deposited in two different reducing atmospheres. Fig. 2(a) exhibit polish-surface micro aggregates for the films produced by CTR. Meanwhile, the film prepared by HR demonstrate mixed nanocluster- and microsphere-like structures, supporting the formation of two phases. The micro clusters are predominantly metallic indium, whereas the microspheres are purely In_2O_3phase.Elemental composition by energy dispersive X-ray (EDX) spectroscopy reveal that the micro-aggregates (Fig. 2(a)) are purely In_2O_3 because of the high O content (51.36 at.%), which is near stoichiometric (60 at.%), indicating full oxidation during growth(Fig. 2(c)).This result support the XRD data (Fig. 1, pattern 'a') where only In_2O_3 can be seen. On the other hand, Fig. 2(b) shows a combination of both metallic indium and In_2O_3materials because of the very low O content (35.87 at.%), suggesting incomplete oxidation of the adsorbed gaseous species (Fig. 2(d)). The impurity Si element comes from the Si substrate. The relatively higher indium content for the film fabricated by HR (Fig. 2(b)) supports the dominance of tetragonal metallic indium phase on the film, as indicated by the presence of strong indium diffraction peak on the XRD result (Fig. 1, pattern 'a').

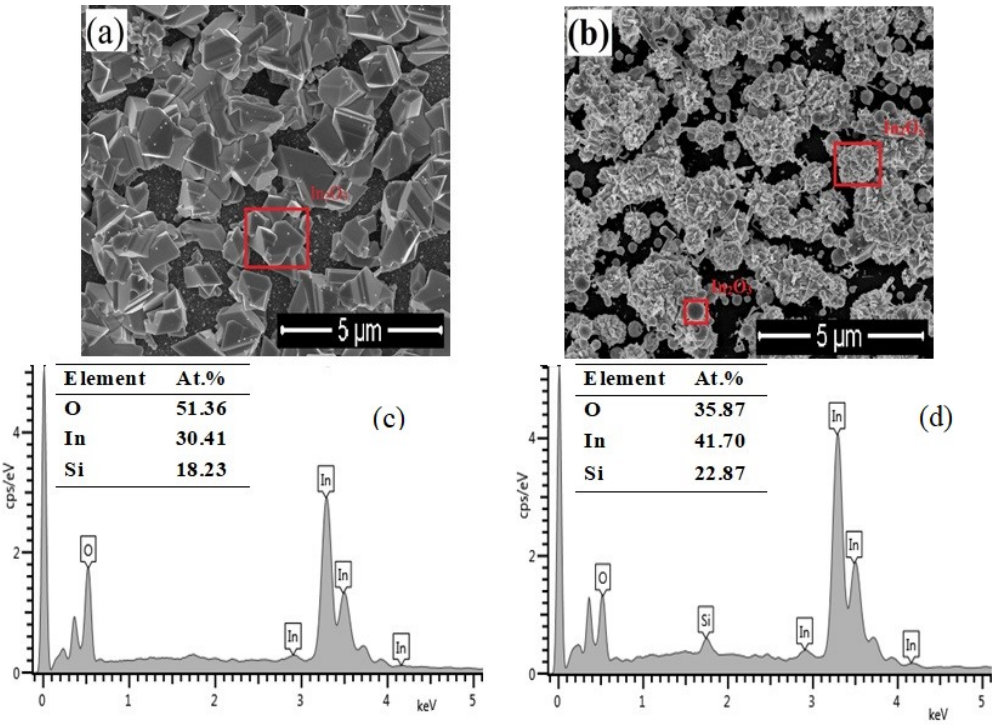

Figure 2. FE-SEM micrographs of the In_2O_3 MSs grown by: (a) CTR, (b) HR; and spectrographs for the films prepared by (c) CTR, (d) HR.

The growth mechanism follows four proposed sequential steps which can be identified in the growth process: (i) reduction of In_2O_3 powder and vapour phase transport of reagent species; (ii) deposition of reagent species onto the substrate followed by nucleation and oxidation; (iii) transfer of absorbed species along the surface of nucleation; and (4) growth into super saturated MSs (Fig. 3).The first step being the CTR or HR of In_2O_3 powder into volatile species at high temperature may occur according to Eqs. 1 & 2. The carbon involved in the CTR provides a moderate reducing ambient at high temperature, resulting in the vapourisation of the indium suboxide In_2O (Eq. 1) [11, 12]. Note that CO_2 and CO evolve at < 700 ℃ and ≥ 700 ℃, respectively [11]. However, the indium vapour predominates in the H_2reducing atmosphere during HR due to the stronger reducing environment, leading to the formation of a mixed-phase indium-In_2O_3film (Eq. 2). The drastic reduction of In_2O_3 (s) into In (g), according to Eq. 2, is supported by the prevailing tetragonal metallic indium phase on the XRD pattern 'b' (Fig. 1)

$$In_2O_3(s) + 2C(s) \xrightarrow{850\ ℃} In_2O(g) + 2CO(g) \qquad 1$$

$$In_2O_3(s) + 3H_2(g) \xrightarrow{850\ ℃} 2In(g) + 3H_2O(g) \qquad 2$$

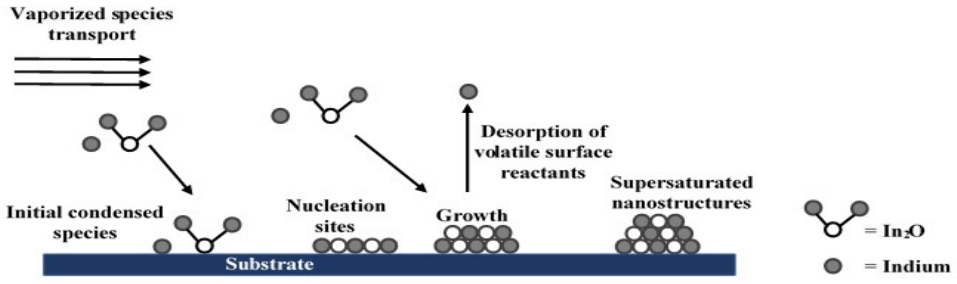

Figure 3. Schematic of the mechanism for the CVD growth process.

In the second step, the vapourised species are transferred and deposited on the substrate by N_2 carrier gas. The initial absorbed gaseous reagents on the substrate undergo oxidation by residual oxygen trapped in the tube [12] and water vapour from the bubbler to form small In_2O_3 nuclei via sublimation (Eq. 3, for the CTR process),and indium-In_2O_3 mixed-phase nuclei (Eq. 4, for the HR process). The small pure In_2O_3nuclei formed by sublimation of In_2O serve as self-nucleation/ or solid nucleation centers to promote the MSs growth and preferred orientation [17] – a process which can be described herein as vapour-to-solid-to-solid growth (for the CTR and deposition process). On the contrary, growth scheme for the mixed-phase film can be described as vapour-to-liquid-to-solid growth for the HR and deposition process. This is because the predominating metallic indium vapour deposits on the substrate and condense into liquid phase before being partially oxidized into the small mixed indium-In_2O_3 nuclei (Eq. 4). The small nuclei now serve as the self-nucleation sites. The indium vapour condenses first into the liquid phase because of its low melting point (430 K at 1 atm.), whereas the In_2O vapour sublime because of its low boiling point (800 K at 1 atm.) [15]. This self-catalytic growth associated with many thermodynamic parameters is a rather complicated process that needs quantitative modeling [17].

$$In_2O(g) + O_2(g) + H_2O(g) \xrightarrow{< 850\,^{\circ}C} In_2O_3(s) + H_2O(g) \quad 3$$

$$3In(g) + O_2(g) + H_2O(g) \xrightarrow{< 850\,^{\circ}C} In_2O_3(s) + In(s) + H_2(g) \quad 4$$

Finally, the small nuclei grow via continuous adsorption of hot reagents, oxidation, and migration of the absorbed species along the surface to the preferred crystallographic planes.

In the interim, the formation of the micro aggregates which is characterized by the pure In_2O_3 phase (Fig. 1, pattern 'a'), and also indicated by the yellowish-white colored film [4, 11] can be due to the In_2O-rich ambient (Eq. 1) observed during the CTR process. The In_2O (g) have some oxygen content so, it can easily get completely oxidized into the supersaturated pure In_2O_3 crystal (Figs. 1 & 2(a)). Only the In_2O_3 microaggregates can be formed in the CRT process because the volatile species is dominated by the suboxide In_2O.

Contrarily, In_2O_3 powder can be directly reduced into indium vapour [4] during the HR process because of the stronger reducing atmosphere (Eq. 2). Therefore, the mass transport of indium vapour in the growth front can result in the formation of indium-In_2O_3 mixed-phase (Fig. 1) in the oxygen-deficient environment. Since the indium vapour is highly deficient in oxygen content, it may require a high amount of oxygen and a longer reaction time to be completely oxidized into the In_2O_3 phase. This can be the reason why the film produced by HR process comprise of the microcluster- and microsphere-like structures which are predominantly metallic indium and In_2O_3 phases, respectively [16] (Fig. 2(b)). The presence of the metallic indium phase can be evidenced by the gray appearance of the film produced by HR [16]. The HR technique has proved to be inappropriate for fabricating pure In_2O_3 crystals. Additionally, the indium vapour evolved during the HR process can lead to the corrosion of the metal flanges of the furnace. CTR is therefore, proposed as the feasible reduction process for the evaporation and deposition of pure In_2O_3 crystal via the CVD method.

Optical characterization

Fig. 4 demonstrates optical reflectance results of the prepared In_2O_3 nano materials. The oxide semiconductor materials exhibit cut-off wavelengths ~404 and ~322 nm near the optical absorption edge for the films produced by CTR and HR, respectively (Fig. 4(a)).

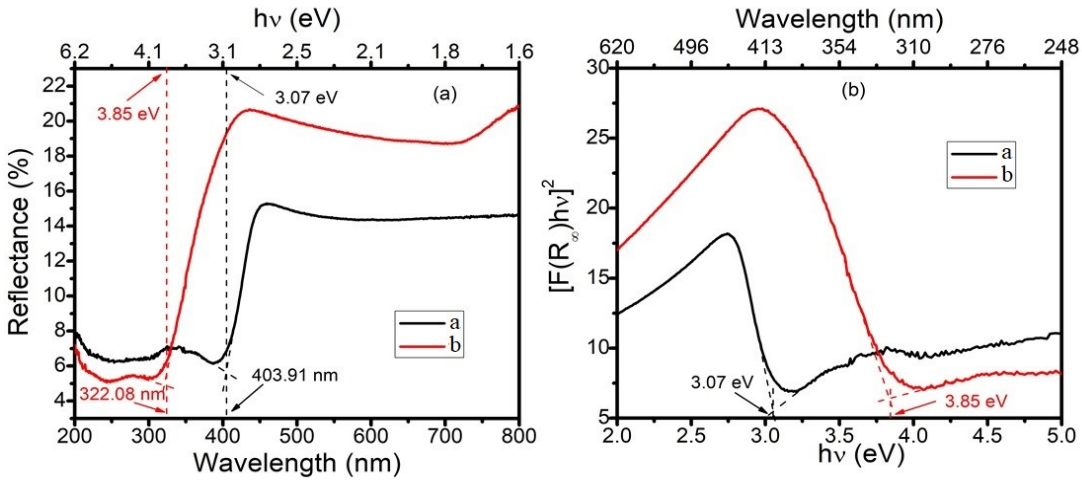

Figure 4. (a) Optical reflectance spectra of In_2O_3 MSs produced by CTR and HR; (b)Tauc plot

The cut-off wavelengths correspond to the optical band gaps (E_g) 3.07 and 3.85 eV for the CTR- and HR-grown films, respectively (Fig. 4(a)).Tauc plot (Fig. 4(b)) produced according to the Tauc, Davis and Mott method [5, 18] lead to an extrapolation of the E_g using a based line [19]. The E_g values are determined to be 3.07 and 3.85 eV for the films produced by CTR and HR, respectively. The larger E_g value for the film produced by HR can be attributed to the interface between the indium-In_2O_3 mixed-phase [13], and the smaller D 53.13 nm. Meanwhile, the E_g values obtained from the Tauc (Fig. 4(b)) agree with those estimated from the raw reflectance data (Fig. 4(a)), and are consistent with literature [4, 5, 20].

Conclusion

In summary, pure In_2O_3 crystal and indium-In_2O_3mixed-phasefilms were deposited by the CTR and HR processes, respectively via CVD method. The pure In_2O_3 film exhibited microaggregate-like morphology whereas, the mixed-phase indium-In_2O_3 crystal system showed mixed microcluster and microsphere-like morphology. The pure In_2O_3 film had a near-stoichiometric oxygen content whereas, the mixed-phase film had relatively low and higher oxygen and indium contents, respectively. Optical band gap was found to be 3.07 and 3.85 eV for the films prepared by CTR and HR processes, respectively. The CTR has been proposed in this study as the feasible reduction technique for the evaporation and deposition of pure In_2O_3 crystals by the CVD method. The CTR technique is a cost-effective and safest process as compared to the HR, based on the cost of the various reducing agents and handling procedure. The prepared materials can be applied for chemical sensing and UV photo detection.

Acknowledgment
The authors would like to thank Universiti Sains Malaysia (USM) and the Fundamental Research Grant Scheme (FRGS: 203.PFIZIK.6711900) from *Kementerian Pengajian Tinggi* (KPT), Malaysia for their technical and financial support for this work.

Declaration of conflicting interests

The authors declared no potential conflicts of interest

References

[1] Faisal, A.D. Aljubouri1, A.A .and Khalef, W.K. 2020. **Synthesis of indium oxide nanowires on quartz substrate for gas sensor** .*Journal of Applied Science and Engineering*23(3),461–468.

[2] Qurashi, A. El-Maghra by, E.M. Yamazaki, T. andKikuta, T. 2010. **Catalyst supported growth of In_2O_3 nanostructures and their hydrogen gas sensing properties**. *Sensors and Actuators B: Chemical*147(1),48–54.

[3] Yan, Y.-G. Zhang, Y. Zeng, H.-B. and Zhang, L.-D. 2007. **In_2O_3Nanotowers: controlled synthesis and mechanism analysis**. *Crystal Growth and Design* 7(5), 940–943.

[4] Karn, A.Kumar,N. and Aravindan, S. 2017.**Chemical vapour deposition synthesis of novel indium oxide nanostructures in strongly reducing growth ambient.** *Journal of Nanostructures* 7(1),64–76.

[5] Aper, T.M. Yam, F.K. Poay, B. K. andJubu, P.R. 2020. **Morphological and structural transformations of indium oxidenano structures in ammonia growth ambient by atmospheric chemical vapour deposition**. *Materials Sciencein Semiconductor Processing* 118,1–8.

[6] Pan, Z.W.Dai, Z.R. andWang, Z.L. 2001. **Nanobelts of semiconducting oxides**. *Science* 291, 1947–1948.

[7] Li, Y. Bando, Y. and Golberg, D. 2003. **Single-Crystalline In_2O_3 nanotubes filled with In**. *Advanced Materials* 15(78), 581–585.

[8] Kumar, M. Chatterjee, R. Milikisiyants, S. Kanjilal, A. Voelskow, M. Grambole, M. andSingh, J.P. 2009. **Investigating the role of hydrogen in indium oxide tubular nanostructures as a donor or oxygen vacancy passivation center**.*Applied Physics Letters* 95(1),1–7.

[9] Yang, W. Wan, P. Meng, H. Hu, J. andFeng, L. 2015. **Super saturation-controlled synthesis of diverse In_2O_3 morphologies and their shape-dependent sensing performance**. *Cryst. Eng. Comm.* 17(15), 2989–2995.

[10] Liu, Z. Yamazaki, T.Shen, Y.Kikuta,T.Nakatani, N. andLi, Y.2008. **O_2 and CO sensing of Ga_2O_3 multiple nanowire gas sensors**. *Sensors and Actuators B* 129, 666–670.

[11] Xiangfeng, C. Caihong, W.Dongli, J. andChenmou, S. 2004. **Ethanol sensor based on indium oxide nanowires preparedby carbothermal reduction reaction.** *Chemical Physics Letters* 399, 461–464.

[12] Singh, N. Zhang, T. andLee, P.S. 2009. **The temperature-controlled growth of In_2O_3nanowires, nanotowers and ultra-long layered nanorods**. *Nanotechnology* 20(19), 1–9.

[13] Nistor, M. Seiler, W, Hebert, C. Matei, E. and Perrière, J. 2014**. Effects of substrate and ambient gas on epitaxial growth indium oxide thin films**.*Applied Surface Sciences* 307, 455–460.

[14] Tuzluca, F.N.Yesilbag, Y.O.and Ertugrul, M.2018. **Synthesis of In_2O_3 nanostructures with different morphologies aspotential**

supercapacitor electrode materials.*Applied Surface Sciences* 427,956–964.

[15] Yadav, K. Mehta, B.R. and Singh, J.P.2014.**Template-free synthesis of vertically aligned crystalline indium oxide nanotube arrays by pulsed argon flow in a tube-in-tube chemical vapour deposition system**. *Journal of Materials Chemistry C* 2(31), 6362–6369.

[16] Guenther, G. Schierning, G. Theissmann, R. Kruk, R. Schmechel, R. Baehtz, C. andProdi-Schwab, A. 2008. **Formation of metallic indium-tin phase from indium-tin-oxide nanoparticles under reducing conditions and its influence on the electrical properties**. *Journal of Applied Physics* 104(3), 034501–8.

[17] Lu, J.G.Chang, P.and Fan, Z.2006. **Quasi-one-dimensional metal oxide materials—Synthesis, properties, and applications**. *Materials Science and Engineering R* 52, 49–91.

[18] Jubu, P.R. Yam, F.K. and Low, K.T. 2020. **Feasibility study on synthesis of gallium oxide nanostructures on glass substrate by chemical vapour deposition**. *Thin Solid Films* 710,1–7.

[19] Jubu, P.R. Yam, F.K. Igba, V.M.and Beh, K.P. 2020. **Tauc-plot scale and extrapolation effect on bandgap estimation fromUV–vis–NIR data – A case study of β-Ga_2O_3**. *Journal of Solid State Chemistry* 290, 1–10.

[20] Girtan, M. and Folcher, G. 2003. **Structural and optical properties of indium oxide thin films prepared by an ultrasonic spray CVD process**. *Surface and Coatings Technology* 172(2-3),242–250.

Cite this article

Jubu P.R., Aper T.M. and Igba V.M. (2021). Growth Mechanism and Structural Elucidation of Indium Oxide Microstructures Prepared by Carbo-thermal and Hydrogen Reduction Processes. *FUAM Journal of Pure and Applied Science*,**1**(**1**): 20-26